Available online at www.sciencedirect.com
ScienceDirect
C. R. Mecanique 335 (2007) 342–350
COMPTES RENDUS MECANIQUE
http://france.elsevier.com/direct/CRAS2B/

Melting and solidification: processes and models/Experiments for solidification benchmarks

Geometry of the melting interface in cylindrical metal rods under microgravity conditions

Nicolas R. Ward, Ted A. Steinberg *

School of Engineering Systems, Faculty of Built Environment and Engineering, Queensland University of Technology, Brisbane, Australia

Available online 22 June 2007

Abstract

The melting interface geometries present within cylindrical iron rods in microgravity are examined. Melting samples are quenched in microgravity by immersion in a water bath. Samples are sectioned on multiple planes and photo microscopy analysis is used to determine the shape of the melting interface on each plane. Images from multiple cross-sections are assembled to produce a three-dimensional representation of the melting interface present in microgravity. Iron rods are shown to have an asymmetric, convex melting interface in microgravity, with a significantly different (increased) heat transfer area compared to the planar normal-gravity case. The change in surface area of the melting interface between normal gravity and microgravity is shown to provide excellent agreement with the observed change in melting rate, as predicted by simple one-dimensional heat transfer analysis. ***To cite this article: N.R. Ward, T.A. Steinberg, C. R. Mecanique 335 (2007).***

Résumé

Géométrie de l'interface de fusion dans les barreaux cylindriques en microgravité. Les formes d'interface de fusion présentes dans les barreaux cylindriques d'acier en microgravité sont examinées. Des échantillons fondus sont refroidis en microgravité par immersion dans un bain d'eau. Les échantillons sont sectionnés en de multiples plans et l'analyse de photo de microscopie est employée pour déterminer la forme du front de fusion dans chaque plan. Des images des sections transversales multiples sont assemblées pour produire une représentation tridimensionnelle de l'interface de fusion en microgravité. Il est trouvé que des tiges de fer conduisent à une interface de fusion asymétrique et convexe en microgravité, avec une surface de transfert thermique accrue par comparaison au cas plan en pesanteur normale. Le changement de la superficie de l'interface de fusion entre la pesanteur normale et la microgravité est en excellent accord avec le changement prédit par une analyse unidimensionnelle simple du transfert thermique. ***Pour citer cet article : N.R. Ward, T.A. Steinberg, C. R. Mecanique 335 (2007).***

Keywords: Fluid mechanics; Melting interface; Melting rate; Burning metals; Quench; Microgravity; Melting surface geometry

Mots-clés : Mécanique des fluides ; Interface de fusion ; Taux de fusion ; Métaux combustibles ; Microgravité ; Topologie de la surface de fusion

1. Introduction

The melting of metallic materials is an important process from both a fundamental scientific viewpoint and in many industrial applications. Many disciplines require knowledge about the melting characteristics of metallic materials to

* Corresponding author.
E-mail address: t.steinberg@qut.edu.au (T.A. Steinberg).

1631-0721/$ – see front matter
doi:10.1016/j.crme.2007.05.008

provide a fundamental understanding of the processes being characterised or improved. These disciplines include materials processing (encompassing both base metal/alloy production and specific component manufacturing), fire-safety of metallic materials (typically in oxygen systems), and combustion synthesis processes.

It has been noted in previous microgravity work that the melting rates for cylindrical metal rods are significantly higher than those observed under similar conditions in normal gravity [1–5]. This is problematic for the designers of spacecraft and orbital materials processing equipment because the application of normal-gravity melting data in microgravity is highly non-conservative and often not valid [2]. The cause of higher melting rates for metallic materials in microgravity is not well characterised. However, earlier work suggested that, in microgravity, altered interfacial geometry between the solid and liquid metal could result in higher heat transfer rates with associated faster melting [6,7]. It is necessary to characterise the cause of the observed differences in melting rates as a function of gravity level to improve the fundamental scientific understanding of this phenomenon. This knowledge is required to improve both ground-based and space-based applications involving materials processing and fire-safety. Since the specific goals of the current space programs of several nations include expansion of human presence in orbit, establishment of lunar bases and wider exploration, these applications are expected to become even more important, making the understanding of the changes in melting rates of metallic materials due to gravitational variations highly relevant. Therefore, more information about the melting interface established within a melting metallic sample in microgravity is required. The objective of this investigation is to improve the understanding of how metallic materials melt in microgravity by determining the geometry of the melting interface that is formed under these conditions.

2. Background

One method to determine the rate at which a metallic material melts is to use a standard test typically used to evaluate its flammability. Three such tests are currently used, produced by NASA [8], ASTM [9], and ISO [10]. In all of these tests, a vertically mounted (typically 3.2-mm diameter) cylindrical rod of the material under investigation is ignited in an environment that will support self-sustained burning, or rapid oxidation. Energy released by the metal oxidation reactions is transferred to the solid test specimen, causing melting. Since most metallic materials burn heterogeneously [11], burning typically occurs within a molten drop which forms and is attached to the solid test specimen at the melting interface. In normal gravity, the melting interface has been shown to be planar and perpendicular to the rod centreline [12]. The Regression Rate of the Melting Interface (RRMI) is defined as the rate at which the melting interface proceeds along the test specimen. In normal gravity, as the sample rod melts, the size of the molten drop increases until its weight exceeds the adhesion and surface tension forces holding it to the solid rod. At this point, the drop detaches from the rod and a new drop growth-and-detachment cycle begins. In microgravity, detachment does not occur; instead, a spherical liquid drop remains attached to the solid rod throughout the test and grows in size [3]. For commercially pure iron, the RRMIs observed in microgravity are 1.5 to 2.0 times higher in microgravity than in normal gravity [2–7]. Although the differences relative to normal-gravity melting rates vary between metallic materials, higher melting rates, by factors of up to 4 and 5, have also been observed in microgravity for other metals and alloys (aluminium, stainless steel, etc.) [3].

Previous work has indicated that the rate of heat transfer between the liquid and solid phases at the melting interface may be the mechanism which limits the RRMI in the standard test configuration in normal gravity [13]. In addition, tests involving melting cylindrical iron samples during a transition in gravity level from normal gravity to microgravity also suggested that the geometry of the melting interface changes and will strongly influence the observed RRMI. In these tests, a sudden increase in RRMI occurred at the onset of microgravity, correlated with the sudden change in the geometry of the molten drop from a tear drop shape (stretched by gravity) to that of a near perfect spherical shape (without gravity induced stretching). It was hypothesised that the change in shape of the attached molten drop, induced by a reduction in the gravity level, altered the internal geometry of the molten system, resulting in a convex melting interface. This new shape, significantly different to the typically planar melting interface observed in normal gravity, would result in an increased contact area between the liquid and solid phases [6,7]. Theoretical analysis indicated that a larger melting interfacial surface area allows increased heat transfer, thus offering a possible explanation of the higher RRMIs observed in microgravity. The theoretical analysis was based on a one-dimensional energy balance at the melting interface and is shown in Eq. (1) [7]. Eq. (1) shows the RRMIs dependence on boundary temperatures (the reaction temperature, T_R, the melting temperature, T_M, and the ambient temperature, T_0), thermo-physical properties (density, ρ, thermal conductivity, k, heat of fusion, λ, and specific heat C_P), and the ratio of melting interface surface

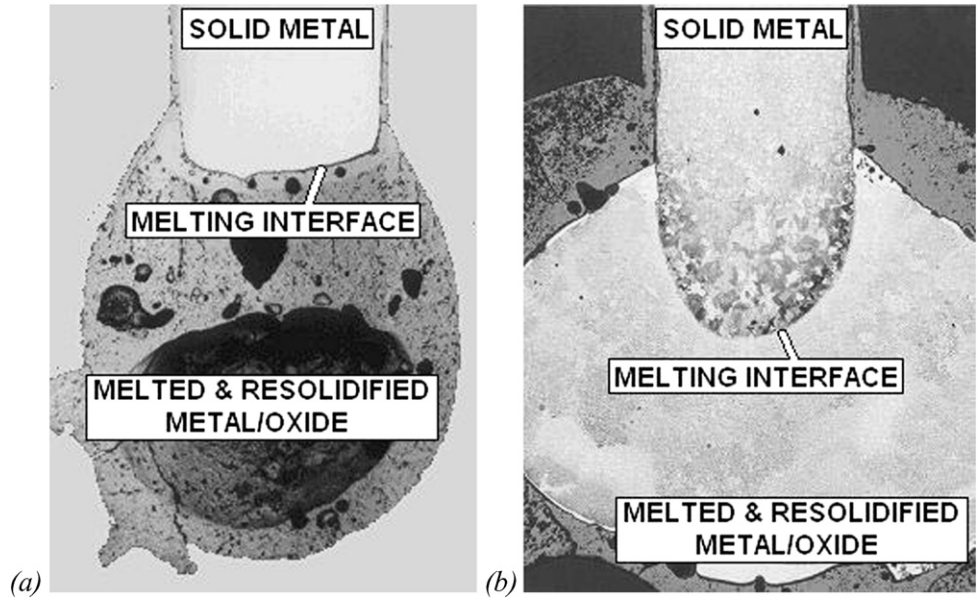

Fig. 1. Cross-sections of 3.2-mm diameter iron rods, burned in (a) normal gravity and (b) microgravity. Note melting interface shapes [14].

Fig. 1. Sections transversales des tiges de fer de 3,2 millimètres de diamètre, brûlées sous des conditions de (a) pesanteur normale et (b) microgravité. Notez les formes du front de fusion [14].

area to rod cross-sectional area, A_{MI}/S. The analysis shows that a change in RRMI will be proportional to a change in the area ratio, A_{MI}/S, for all other parameters constant. However, this theoretical result can only be confirmed by incorporating a known microgravity melting interface area into the heat transfer model allowing correlation of the heat transfer surface area with experimentally observed RRMI values. Therefore, to validate the proposed mechanism for the increased RRMI's observed the exact geometry of the melting interface in microgravity is required.

$$\mathrm{RRMI} = \frac{A_{\mathrm{MI}}}{S}\left[\frac{k}{\Delta x}\frac{1}{\rho}\frac{(T_R - T_M)}{[c_P(T_M - T_0) + \lambda]}\right] \tag{1}$$

A cross-section of a post-test specimen of iron that melted in normal gravity is shown in Fig. 1(a). The melting interface is approximately planar and perpendicular to the centreline of the test sample. The cross-section of a similar sample obtained in microgravity is presented in Fig. 1(b). The melting interface is clearly not planar, but has a convex shape. However, these images cannot be presented with confidence, as both samples were allowed to cool slowly to room temperature, and significant geometric changes may have occurred before the sample was completely solidified [14]. Therefore, this image may not be representative of the microgravity melting interface that is actually present during melting. Samples which are more representative of the melting interface can be obtained by rapidly quenching the molten system, by immersing the sample rod in water as melting occurs [15]. However, obtaining rapidly quenched samples in microgravity is a non-trivial problem with several associated experimental difficulties.

3. Approach

Commercially pure (3N purity, 99.9%) 3.2-mm-diameter iron rods were burned in 99.95% pure oxygen at pressures ranging from 2.1 to 6.2 MPa (300 to 900 psia). A high pressure combustion chamber, shown in Fig. 2(a) and described in earlier work [7], was used for all experiments. The microgravity environment was provided in a 2-s duration drop tower operated by Queensland University of Technology in Brisbane, Australia. The microgravity facility and its performance are described in earlier work [16,17]. Six tests were performed with representative samples subjected to photo microscopy analysis to determine the exact geometry of the melting interface.

Test samples were ignited by resistively heating a thin fuse wire. After ignition, the molten system produced during self-sustained burning (oxidation) was rapidly quenched by immersing the sample in water. In Tests 1 and 2, the sample was immersed in water during microgravity, and in Tests 3 to 6, immersion occurred at the end of

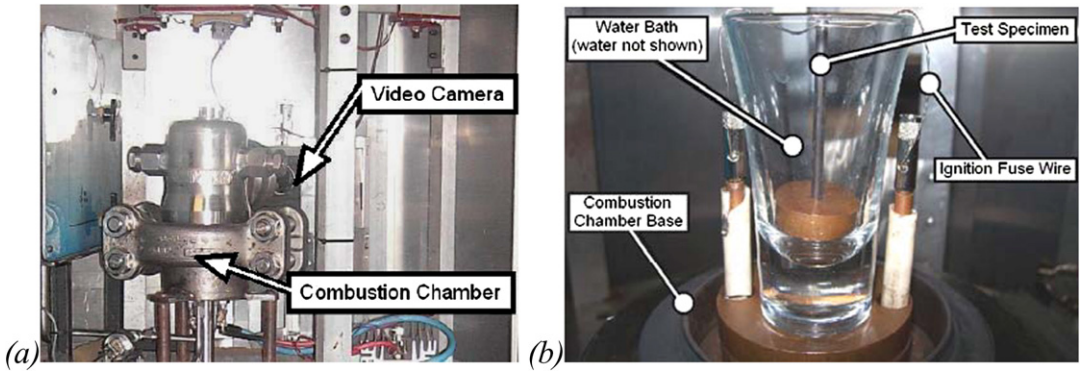

Fig. 2. Apparatus, including (a) combustion chamber system, and (b) test specimen configuration incorporating microgravity quench system.
Fig. 2. Appareillage incluant (a) chambre de combustion, et (b) configuration d'essai de trompe en microgravité.

Table 1
Observed RRMIs (melting rates) from video analysis
Tableau 1
RRMI obsérvés (taux de fusion) depuis l'analyse video

Test	Quench	O_2 pressure (MPa)	RRMI (mm/s)
1	During microgravity	5.86 ± 0.03	17.0 ± 1.7
2		6.16 ± 0.03	16.1 ± 1.6
3	During deceleration	2.4 ± 0.3	14.2 ± 1.3
4		2.4 ± 0.3	14.1 ± 1.3
5		2.1 ± 0.3	11.8 ± 1.0
6		2.4 ± 0.3	14.0 ± 1.3

microgravity conditions, when the experiment came to rest at the bottom of the drop tower. Test sample immersion was achieved with an *upside down* variation of the standard experimental configuration. The test sample was mounted to protrude vertically from a water bath, as shown in Fig. 2(b). In this configuration, the sample was ignited at the top and melted downward along the rod until the molten material entered the water where it was rapidly quenched. The required sample rod length above the water was estimated from the product of an expected RRMI (based on previous microgravity test results at similar pressures) and the desired burn duration necessary to contact the water prior to, or at, the test conclusion as required.

4. Results

The microgravity levels used during test were less than 10^{-2} g; this being the resolution limit of the accelerometer used, however, theoretical analysis suggests g-levels less than 10^{-4} g were present. Peak deceleration loads at the conclusion of a test were 17 ± 1 g. Images taken from the video of Test 3 are presented in Fig. 3 and show ignition and subsequent downward melting of the sample in microgravity. The RRMI is determined by post-test visual analysis of the video data with the results summarised in Table 1. Errors in time measurement, video scale factor and user input were summed in quadrature to estimate the total error in RRMI.

5. Analysis

Photo microscopy analysis was performed to determine the geometry of the melting interface. Test specimens were mounted in resin blocks and, for each sample, this block was then ground away using sandpaper, until a planar cross-section of the sample was exposed. This surface was then polished and etched with 2% Nital solution, to reveal the local grain structure of the specimen. The exposed surface was then photographed through an optical microscope, under crossed-polarised light with a 1/4 wavelength filter. Images obtained in this way were then assembled into a

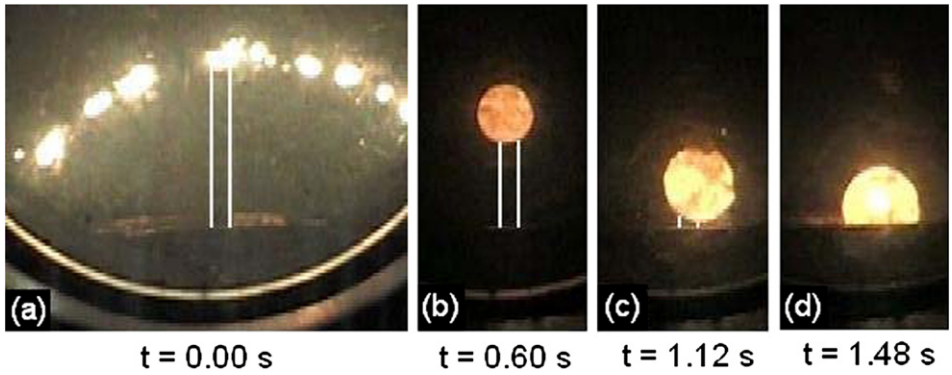

Fig. 3. Iron melting in microgravity, including (a) ignition of fuse wire, (b) and (c) subsequent growth of the attached molten drop, and (d) entering the quench cup (white lines show location of 3.2-mm diameter test specimen).

Fig. 3. Clichés de fusion d'acier en microgravité, incluant (a) amorcage, (b) et (c) séquences de croissance de la bulle fondue attachée et (d) pénétrant le bain (les lignes montrent l'emplacement 3.2-mm de diamètre).

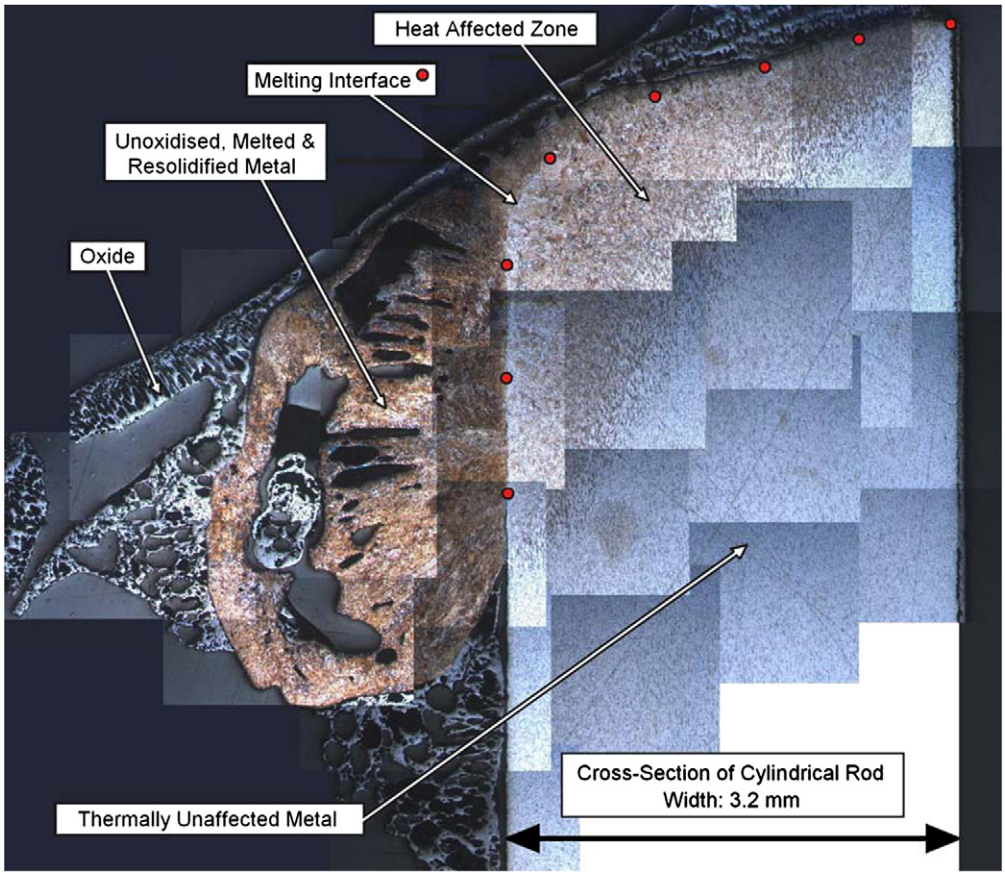

Fig. 4. Typical cross-section mosaic image (from Sample 6, Cut 3).

Fig. 4. Section transversale typique en image mosaique (à partir de l'échantillon 6, coupe 3).

single mosaic, as shown in Fig. 4. The melting interface was identified as the boundary between the heat affected zone and the region that melted and resolidified. This process was repeated several times per sample, to expose and photograph multiple, successively deeper cross-sections. The mosaic images from each cross-section were assembled to build a valid three-dimensional representation of the actual geometry of the melting interface.

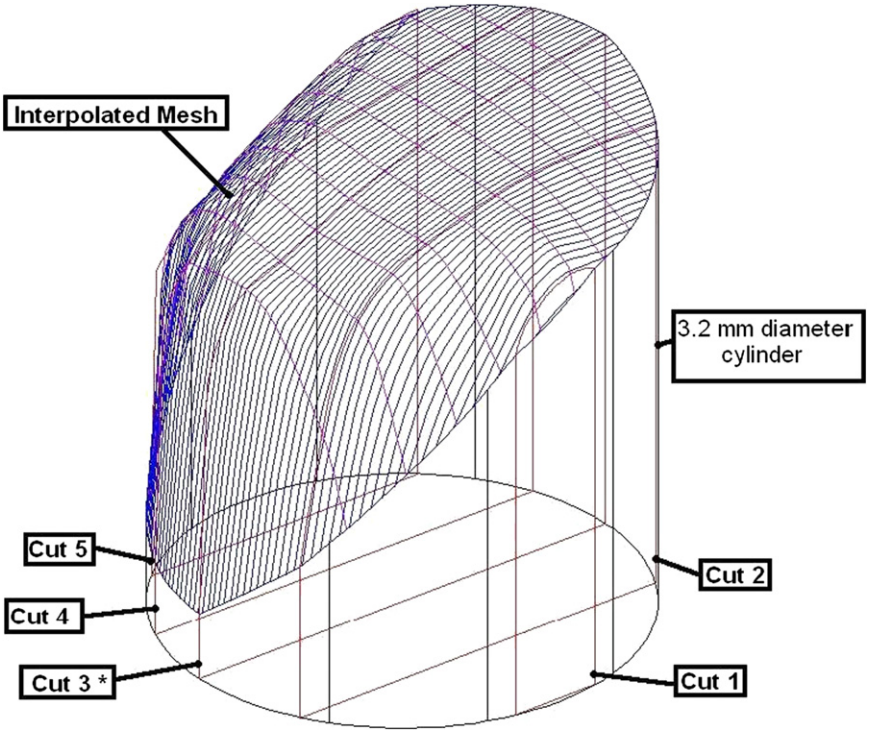

Fig. 5. Model of the melting interface for Sample 6. Cut 3 obtained from Fig. 4.

Fig. 5. Modèle d'interface de fusion pour l'échantillon 6. Coupe 3 obtenue à partir de la Fig. 4.

The depth of each parallel cross-section was obtained by measuring the width of the exposed rod surface, and representing this line as a secant on the original cylindrical sample. Mosaic images were then aligned using a reference point, common to all cross-sections. Matlab® was used to map the three-dimensional surface across and between the two-dimensional melting interface geometries identified at each cross-section. Interpolation was performed using cubic splines and the final mesh drawn with 0.05-mm line spacing. A typical three-dimensional melting interface geometry determined in this way (for Test 6) is shown in Fig. 5. The area of the melting interface shape defined in this way was calculated by performing a numerical integration over the surface. To verify this technique, the method was used to find the area of a hemispherical surface. The numerical method matched the exact analytical solution to within 2%, verifying the numerical integration technique. However, this value does not represent the total error associated with the surface area estimate. Other sources of error are present in the image interpretation process, although these have not been quantified. For the sample shown, the melting interface surface area was determined to be 14.6 mm^2.

6. Discussion

It is necessary to validate the use of a downward burning configuration, as this is generally avoided in normal gravity due to the uncontrollable and unreproducible movement and regression of the molten material, which tends to flow down the side of the test sample. To avoid this, the standard tests require that samples are melted from the bottom upwards, which allows "*molten slag … to fall away from the test specimen, giving more reproducible results*" [18]. However, in microgravity, drop detachment does not occur, so the flow of molten material is not a concern. This is consistent with the fact that, in the absence of a gravitational vector, there is no up or down, so there is no difference between upward and downward configurations during melting of a solid rod in microgravity. This conclusion is validated by comparison of RRMIs obtained in both an upward and downward configuration in microgravity for similar test conditions. In an upward burning configuration under similar test conditions, the RRMI for a 3.2-mm-diameter iron rod at 2.1 MPa (300 psia) was 14.3 ± 0.4 mm/s, an average of five tests [7]. In the

downward burning configuration used in this investigation, the observed RRMI at 2.4 MPa (350 psia) was similar, at 14.1 ± 1.3 mm/s. This result supports the validity of a downward burning configuration in microgravity.

It is also necessary to verify that the samples obtained are representative of the melting occurring in microgravity, that is, the cooling times were sufficiently short. Samples can be considered representative only if no significant changes in melting interface geometry occur during the solidification process. This primarily requires a rapid cooling time. During Tests 1 and 2, in which the burning system was immersed in water during microgravity, the surface remained highly luminous for the whole microgravity period, a duration exceeding 1.4 s. The luminosity was only reduced upon impact at the bottom of the drop tower. This surprisingly long cooling time is attributed to decreased heat transfer rates between molten combustion products and water, due to film boiling at the surface of the molten mass (that was clearly visible on the video recordings). Over the short duration tests performed, the film boiling phenomenon appears to have been stable in microgravity. This has not been observed during quench tests in normal gravity [15]. Accordingly, the cooling time for these two tests was considered too long, and these samples were excluded from the post-test analysis.

All other tests (Tests 3 to 6) produced samples that were quenched immediately at the end of the microgravity period. A simple lumped capacitance calculation, using published thermo-physical data for liquid iron and water, was used to estimate the cooling time after impact. The predicted cooling time was 0.05 s, which was verified by video by the associated drop in luminosity within two frames (0.04 s). In the experiments conducted here, cooling occurred in high gravity, peaking at 17 g indicating natural convection would be more effective at cooling the molten sample, making the quench times far faster than in normal gravity or microgravity. In addition, the high gravity environment rapidly removes most of the molten material from the melting interface while not permitting further melting to occur. This further reduces cooling times by rapidly transporting thermal energy away from the melting interface. Therefore, the melting interface geometries obtained through microanalysis of samples from Tests 3 to 6 are considered representative of the actual geometry typically present in the microgravity environment.

The technique used to determine the three-dimensional geometry of the melting interface requires fewer simplifying assumptions than previous investigations that have typically been performed only on a single observation of the specimen mid-plane [14,15]. In these cases, an assumption of axis-symmetry was used in order to draw conclusions about the three-dimensional shape of the melting interface from a single two-dimensional image. In the analysis presented here, the post-test specimens have been analysed on multiple planes, building a far more accurate representation of the three-dimensional geometry of the melting interface leading to a more accurate representation of its actual surface. Though the axis-symmetric assumption is more valid in normal gravity, due to the planar nature of the melting interface, in microgravity, helical motion of the molten drop is often observed, resulting in a highly asymmetric melting interface [2,4]. The technique used in this analysis has the advantage of capturing this asymmetry that is inherent in the microgravity system.

The analysis presented (Fig. 4) reveals that the shape of the melting interface in microgravity is significantly different to the normal gravity case. The melting interface in microgravity is neither planar nor perpendicular to the rod centreline. Instead, in microgravity the melting interface is asymmetric and convex with a larger associated area. This is attributed to wetting of the solid by the molten mass, due to surface tension effects between the liquid metal and solid rod, consistent with earlier observations and conclusions [1,14]. The high surface tension of the molten mass is apparent in previous microgravity results and produces some interesting effects such as continued melting after impact and deceleration [1,6,7]. During these brief, high gravity periods, with peak loads of 17 to 100 g, some molten material remained attached to the solid rod, providing a heat source for continued melting and burning. Further, when samples were ignited at their lengthwise midpoint in microgravity, an unrestrained end was "*rapidly drawn into the molten ball*" [1], consistent with surface tension induced wetting. Thus, in the absence of gravity, surface tension is the dominant force acting on the liquid metal causing the liquid to wet (or engulf) the solid rod. This process alters the interfacial geometry between solid and liquid phases producing the convex melting interface shape observed in post-test analysis.

Heat transfer analysis (Eq. (1)) indicates that a proportional relationship exists between RRMI and the ratio of melting interface surface area to rod cross-sectional area, A_{MI}/S [7]. For 3.2-mm-diameter iron rods melting in normal gravity at 2.4 MPa (350 psia), the RRMIs were 8.2 ± 0.2 mm/s, averaged from five tests [6,7]. In microgravity testing performed here for the same conditions, the observed RRMIs were 14.1 ± 1.3 mm/s, which is 1.6 to 1.9 times faster than in normal gravity. The surface area of the melting interface in normal gravity is simply the circular rod cross-sectional area, 8.04 mm^2. The calculated surface area of the melting interface obtained in this investigation, based

on post-test sample microscopy, is 14.6 mm^2. Therefore, the melting interface surface area was 1.8 times larger in microgravity than in normal gravity which correlates extremely well with the 1.6 to 1.9 times increase in RRMI observed. This provides strong support for the hypothesis that the increase in observed RRMI in microgravity is proportional to the increase in melting interface surface area.

In contrast, similar analysis performed on the slowly cooled microgravity sample shown in Fig. 1(b) indicates that its melting interface surface area is approximately 19.4 mm^2; over 2.4 times larger than the normal-gravity area, which disagrees with the proportional relationship proposed. This clearly demonstrates that an extended cooling time allows further melting to occur during the solidification process. Therefore, rapidly quenching molten samples is necessary to obtain specimens which are representative of the molten system in microgravity.

It remains to be shown whether the results observed for iron apply generally to all metallic materials melting under microgravity conditions. However, it would be expected, due to the high surface tension of liquid metals, that similar wetting phenomena will occur and produce a larger associated melting interface area. This fact is clearly supported by the experimental observation that all the metallic materials tested in microgravity melt faster. Therefore, it is also likely that asymmetric, convex melting interface shapes are present for these metals in microgravity. However, due to differences in specific surface tension values for various metallic materials, it is probable that the extent to which metals are affected by this phenomenon will vary. This is consistent with the large variation in observed melting rates for different metallic materials burning in microgravity [3], especially in comparison to their normal gravity melting rates. It is important to note that changes in reaction phase, reaction chemistry, or other physical and chemical processes may also account for the differences in melting rates for other metallic materials. Further investigation on the influence of gravity level on melting rates for other metals is recommended, especially for metals commonly used in aerospace applications.

7. Conclusions

The geometry of the melting interface for iron rods melting in microgravity was investigated. A novel quench apparatus was developed, enabling the first ever use of water to rapidly cool burning metals in a microgravity system. It is shown that iron has an asymmetric, convex melting interface in microgravity, caused by wetting phenomena driven by high surface tension forces. Similar melting interface geometries are predicted for other metallic materials in microgravity. The relative change in melting interface surface area closely matches the relative change in melting rate between normal gravity and microgravity as predicted by one-dimensional heat transfer analysis. It is concluded that the increase in contact area between solid and liquid phases at the altered melting interface in microgravity causes more heat transfer and subsequent faster sample melting. This investigation has contributed to an improved understanding of heterogeneous burning by revealing the geometry of the melting interface in microgravity.

References

[1] T.A. Steinberg, The combustion of metals in gaseous oxygen, PhD Thesis, Mechanical and Electrical Engineering, New Mexico State University, Las Cruces, NM, 1990.
[2] T.A. Steinberg, D.B. Wilson, F.J. Benz, Microgravity and normal gravity combustion of metal and alloys in high pressure oxygen, in: Flammability and Sensitivity of Materials in Oxygen-Enriched Atmospheres, vol. 6, American Society for Testing and Materials, 1993, pp. 133–145.
[3] T.A. Steinberg, J.M. Stoltzfus, Combustion testing of metallic materials aboard NASA Johnson Space Center's KC-135, in: Flammability and Sensitivity of Materials in Oxygen-Enriched Atmospheres, vol. 8, American Society for Testing and Materials, 1997, pp. 170–188.
[4] T.A. Steinberg, F.J. Benz, Iron combustion in microgravity, in: Flammability and Sensitivity of Materials in Oxygen-Enriched Atmospheres, vol. 5, American Society for Testing and Materials, 1991, pp. 298–312.
[5] T.A. Steinberg, D.B. Wilson, F.J. Benz, The burning of metals and alloys in microgravity, Combust. Flame 88 (1992) 309–320.
[6] N.R. Ward, T.A. Steinberg, Thermal analysis of iron rods burning in normal gravity and reduced gravity, in: Int. Heat Transfer Conf., Sydney, 2006.
[7] N.R. Ward, T. Suvorovs, T.A. Steinberg, An investigation of regression rate of the melting interface for iron burning in normal gravity and reduced gravity, J. ASTM Int. 3 (4) (2006).
[8] Flammability, odor, offgassing, and compatibility requirements and test procedures for materials in environments that support combustion, NASA Technical Standard, National Aeronautics and Space Administration, 1998.
[9] Standard guide for evaluating metals for oxygen service, in: Annual Book of ASTM Standards, American Society for Testing and Materials, 1992, pp. 101–125.
[10] Determination of upward flammability of materials in pressurized gaseous oxygen or oxygen-enriched environments, Space Systems—Safety and Compatibility of Materials, International Organization for Standardization (ISO), Switzerland, 2003.

[11] T.A. Steinberg, M.A. Rucker, H.D. Beeson, Promoted combustion of nine structural metals in high-pressure gaseous oxygen, in: Flammability and Sensitivity of Materials in Oxygen-Enriched Atmospheres, vol. 4, American Society for Testing and Materials, 1989, pp. 54–75.
[12] T.A. Steinberg, D.B. Wilson, Modelling the NASA/ASTM flammability test for metallic materials burning in reduced gravity, in: Flammability and Sensitivity of Materials in Oxygen-Enriched Atmospheres, vol. 9, American Society for Testing and Materials, 2000, pp. 266–291.
[13] F.J. Benz, T.A. Steinberg, D. Janoff, Combustion of 316 stainless steel in high-pressure oxygen, in: Flammability and Sensitivity of Materials in Oxygen-Enriched Atmospheres, vol. 4, American Society for Testing and Materials, 1989, pp. 195–211.
[14] J.R. DeWit, Investigating the combustion mechanisms of bulk metals through microanalysis of post-Test 3.2 mm diameter metallic rods burned in oxygen-enriched atmospheres, PhD Thesis, Department of Mechanical Engineering, The University of Queensland, St. Lucia, Australia, 2003.
[15] B.P. Osborne, T. Suvorovs, J. DeWit, T.A. Steinberg, Microanalysis of quenched and self-extinguished aluminum rods burned in oxygen, in: Flammability and Sensitivity of Materials in Oxygen-Enriched Atmospheres, vol. 10, American Society for Testing and Materials, 2003, pp. 151–163.
[16] B.P. Osborne, T.A. Steinberg, Experimental investigation into liquid jetting modes and break-up mechanisms conducted in a new reduced gravity facility, Microgravity Science and Technology (April 2006), in press.
[17] N.R. Ward, Phenomena in Microgravity Laboratory Homepage. Available online at: www.bee.qut.edu.au/research/projects/microgravity, 2006.
[18] M.A. Benning, B.L. Werley, The flammability of carbon steel as determined by pressurized oxygen index measurements, in: Flammability and Sensitivity of Materials in Oxygen-Enriched Atmospheres, vol. 2, American Society for Testing and Materials, 1986, pp. 153–170.